# THE STRUCTURE OF MARINE PHYTOPLANKTON COMMUNITIES— PATTERNS, RULES AND MECHANISMS

RALF GOERICKE
Scripps Institution of Oceanography
University of California, San Diego
9500 Gilman Drive
La Jolla, CA 92093-0205

## ABSTRACT

The taxonomic structure of marine phytoplankton communities was studied in nearshore, coastal and offshore environments of the Atlantic, Pacific and Indian Ocean to search for common distributional patterns that might suggest mechanisms controlling these. Contributions of different taxa to total phytoplankton pigment-biomass (TChl *a*) were calculated from concentrations of taxon-specific pigments. In most environments studied, variability of phytoplankton biomass was dominated by diatoms or dinoflagellates, the bloom taxa. The pigment biomass of non-bloom-forming taxa varied as an asymptotic function of TChl *a*. Observed patterns for any taxon were often strikingly similar in different environments but differed significantly between taxa in any one environment. Simple functions were used to describe these patterns, which can be used to predict phytoplankton community structure from TChl *a*. The observed patterns are consistent with predictions derived from a simple conceptual model that suggests that total phytoplankton biomass is generally limited by the availability of a critical nutrient, i.e., by bottom-up forces, but that the biomass of some taxa, particularly picoautotrophs, is controlled by grazers under mesotrophic to eutrophic conditions, i.e., top-down forces. The distribution of cyanobacteria suggests that their population dynamics, unlike those of other taxa, is not tightly lined to the dynamics of their grazers, likely because the latter are grazing concurrently on heterotrophic bacteria.

## INTRODUCTION

The taxonomic structure of the phytoplankton community is an important determinant of ecosystem function with far-reaching implications for the cycling of energy and matter in the marine environment. For example, blooms of coccolithophorids or diatoms differ significantly in their impacts on the export of inorganic carbon or silica, respectively (Smetacek 1999; Tyrrell et al. 1999). Similarly, differences in grazer communities are expected to affect rates of carbon export (Michaels and Silver 1988). However, our realization of the importance of phytoplankton or zooplankton community structure in the marine environment is not complemented by a good understanding of its controls (Verity and Smetacek 1996). In the case of phytoplankton communities our understanding is limited to a more or less qualitative understanding (e.g., Margalef 1978). Most models of phytoplankton communities attempting to elucidate the coexistence of multiple species of algae in the same parcel of water are still at the level of two to four taxa or functional groups (e.g., Anderies and Beisner 2000; Litchman et al. 2006; Friedrichs et al. 2007), even though phytoplankton communities of the open ocean are known to consist of tens to hundreds of species (e.g., Venrick 1982; Venrick 2002). On the other hand, attempts to model the community using multiple groups of phytoplankters (e.g., Bissett et al. 1999; Moore et al. 2002) encounter the problem that the number of parameters that must be parameterized increases approximately with the square of the number of the model's taxa (Denman 2003). Clearly, we are far removed from a solid, mechanistic understanding that would allow us to understand and predict the taxonomic structure of phytoplankton communities.

An alternative approach to the problem is to ask if there are consistent patterns characterizing the distribution and abundance of phytoplankton taxa, i.e., rules that can be used to predict phytoplankton community structure. Indeed, some rules have been known for a long time. The seasonal succession of temperate phytoplankton has often been described as progressing from diatoms to flagellates, i.e., from non-motile to motile species (Smayda 1980) or from sinkers to floaters (Macintyre et al. 1997). Similarly, the variability of phytoplankton biomass in the ocean has often been attributed to larger autotrophs; picoautotrophs are viewed as ever-present, contributing to the background biomass (Chisholm 1992; Li 2002). Goericke (2011) recently tested a set of rules implied by Chisholm's (1992) description of variations of phytoplankton size structure with total phytoplankton biomass and found that these did not hold in the California Current system.

Very detailed studies can be carried out using microscopy; however, this wealth of information on species distributions is rarely complemented by physiological information on all these species. Chemotaxonomy, based on compounds that are specific or even unique for different taxa of microalgae, can alternatively be used to

determine the contributions of those taxa to total phytoplankton biomass. Compounds of choice are carotenoids and chlorophylls (Jeffrey et al. 1997). Some of these groups and their associated pigments are diatoms (fucoxanthin), dinoflagellates (peridinin), some groups of oceanic prymnesiophytes (19'-hexanoyloxyfucoxanthin), cryptophytes (alloxanthin), pelagophytes (19'-butanoyloxyfucoxanthin), chlorophytes (chlorophyll *b*, i.e., Chl $b_1$, and neoxanthin), cyanobacteria (zeaxanthin), and *Prochlorococcus* sp. (divinyl-chlorophyll *a*; i.e., Chl $a_2$). Contributions of different microalgal taxa to pigment biomass, often expressed as total chlorophyll a (TChl *a*, the sum of chlorophyll *a*, i.e., Chl $a_1$, and Chl $a_2$), can in principle be determined from concentrations of these biomarkers (Letelier et al. 1993; Mackey et al. 1996; Goericke and Montoya 1998).

This pigment-based approach was applied to data from the monsoonal Arabian Sea (Goericke 2002) to determine contributions of different photoautotrophs to phytoplankton pigment biomass (henceforth "biomass" for brevity). While these distributions were only weakly related to parameters such as temperature and inorganic nutrients, coherent patterns were observed when the biomass of different taxa was plotted against TChl *a*. Diatoms were the bloom species in this system, dominating phytoplankton biomass at high concentrations of TChl *a*. An abundance threshold also existed for diatoms, i.e., these contributed negligibly to phytoplankton biomass when TChl *a* was less than ~0.25 μg $L^{-1}$. Abundance thresholds were also observed for taxa not forming blooms. Once TChl *a* increased above 1 to 2 μg $L^{-1}$ upper limits were observed for the biomass of most taxa, ranging from 0.05 to 0.5 μg Chl $L^{-1}$. The one exception to those patterns was *Prochlorococcus*, which contributed significantly to total biomass at low levels of TChl *a*, but whose biomass declined when TChl *a* reached high values. These results suggest that, at least in the Arabian Sea, phytoplankton community structure is a predictable function of TChl *a*. Similar patterns were observed for concentrations of taxon-specific pigments in the North Atlantic and Mediterranean Sea (Claustre 1994).

The patterns observed in the Arabian Sea for different microalgal taxa are very similar to those described by Raimbault et al. (1988) for the contribution of different size classes of autotrophs to total autotroph biomass in the Mediterranean (see also Chisholm 1992). Thingstad (1998) presented a simple conceptual model predicting exactly such patterns. The essence of the model is nutrient limitation of total phytoplankton biomass and grazer control of the abundance of all groups, except those forming blooms, once total biomass reaches a critical level. Thus, distributional patterns observed in the Arabian Sea provide empirical support for the model of Thingstad. In order to test the generality of these patterns and the conceptual model of Thingstad, variations of phytoplankton taxon-specific biomass with TChl *a* were analyzed in four other environments: a nearshore environment off San Diego, U.S.A.; the coastal/offshore North Pacific off Southern California; the southern sector of the Indian Ocean; and the Sargasso Sea off Bermuda. Distributional patterns observed in these environments were very similar to those of the Arabian Sea (Goericke 2002), suggesting that phytoplankton community structure in the world's oceans varies predictably as a function of TChl *a* and that community structure is controlled by a balance between bottom-up forces, i.e., the availability of resources, and top-down control, i.e., grazers.

## METHODS

***Sampling and Chromatography.*** Seawater was collected at the pier of the Scripps Institution of Oceanography (Scripps Pier) with Niskin bottles from the top meter of the water column (bottom depth 4 to 7 m) between August 1997 and July 2000 at least twice a week. Samples (1L) were stored in amber bottles and filtered in the laboratory within 3 hours onto a Whatman GF/F filter (Goericke et al. 2000). The filters were stored in liquid nitrogen until analysis on a C8-column based high-pressure liquid-chromatography (HPLC) system (Goericke et al. 2000). In the California Current system (CalCOFI cruises during April and October 1995 and October 1996, Scripps Institution of Oceanography 1997) 2.2 to 4.4 L samples were collected from 2 to 3 depths within the mixed layer. The seawater was filtered and processed as described above. Pigment data from previously published studies were used as well: from the Sargasso Sea (U.S. JGOFS BATS program off Bermuda covering the years 1989 until 1998; data retrieved from the U.S. JGOFS Web site), the temperate, subpolar and polar Southern Indian Ocean between 40 and 60°S and 45 and 65°E (Francois et al. 1993), and the Arabian Sea (U.S. JGOFS Arabian Sea program during the NE and early SW monsoons, i.e., cruises TN43, 49, 54; Goericke, 2002).

***Nutrient Enrichment Experiments.*** During the October 1996 CalCOFI cruise seawater was collected before sunrise by CTD rosette from the mixed layer at CalCOFI stations 93.40, 93.120, 90.53, 87.100, 83.55 and 80.90 and was filled into a carboy and distributed into 2.8 L polycarbonate bottles that had been acid washed and Milli-Q water rinsed. Enrichments were made using 2 μM $NH_4Cl$, 2 μM $NaNO_3$ and 0.4 μM $K_2HPO_4$ as initial enrichments, and untreated samples as a control. Treatments and controls were done in duplicate. Bottles were incubated at 60% ambient light in a Plexiglas incubator, cooled with surface-seawater. Samples for pigment analysis were taken every 24 hours for 3 to 4 days and stored as described above.

***Calculation of taxon-specific biomass.*** The pigment biomass of different taxa was determined from concentrations of taxon-specific pigments as previously described (Goericke and Montoya 1998; Goericke 2002). For the optimization procedure pigment ratios were only constrained to be larger than zero. The independence of derived pigment ratios from initial conditions was tested in each case by using different sets of initial parameters. For the Scripps Pier and the California Current system contributions to TChl *a* by dinoflagellates, diatoms, haptophytes, pelagophytes, "green" algae (i.e., chlorophytes, prasinophytes, etc.), cryptophytes, *Synechococcus* and *Prochlorococcus* were calculated. Contributions of *Prochlorococcus*, dinoflagellates and cryptophytes were estimated directly from concentrations of Chl $a_2$, peridinin and alloxanthin, respectively. Contributions of haptophytes, pelagophytes, diatoms and *Synechococcus* were estimated, respectively, from concentrations of 19'-hexanoyloxyfucoxanthin, 19'-butanoyloxyfucoxanthin, fucoxanthin and zeaxanthin, corrected for contribution by pelagophytes, haptophytes, haptophytes and *Prochlorococcus*, respectively.

Contributions of "chlorophytes" and "prasinophytes" were also determined by including prasinoxanthin in the algorithm. However, prasinophytes did not contribute significantly to phytoplankton biomass in the California Current system as evidenced by very low or zero concentrations of prasinoxanthin. Off the Scripps Pier different groups of "green" algae were present and differentiated as follows: The characteristic pigments of chlorophyta are violaxanthin, neoxanthin and Chl $b_1$; only neoxanthin was used to estimate the contribution of chlorophytes to pigment biomass. Prasinophycean biomass was estimated from prasinoxanthin. Larger, transient contributions of euglenophyceae would be evident from changes in the ratio of Chl *b* and neoxanthin. This ratio however, did not vary systematically with the seasons, nor did it display large transients (data not shown), suggesting that euglenophyceae did not contribute significantly to pigment biomass. Eustigmatophyceae (chromophyta) are characterized by high concentrations of violaxanthin relative to other accessory pigments. Thus their presence can be gauged from high violaxanthin-neoxanthin ratios (V:N-ratio). Indeed, the V:N-ratio reached a value of 35 g $g^{-1}$ during September '97, suggesting that eustigmatophyceae were present during this time. The estimated abundance is shown in Figure 1C (bold line). The eustigmatophycean violaxanthin-Chl *a* ratio was estimated as 0.67 g $g^{-1}$. During the rest of the time series the V:N-ratio varied with the seasons; during February and August average values were 1.7 and 3.4 g $g^{-1}$, respectively (data not shown). Statistical analysis and nonlinear curve fitting were carried out in MS Excel.

## RESULTS

***Scripps Pier.*** Off the Scripps Pier total chlorophyll *a* (TChl *a*, i.e. the sum of Chl $a_1$ and Chl $a_2$) ranged from 0.4 to 11 μg $L^{-1}$ with an average value of 2.2 μg $L^{-1}$ for the study period, August 1997 to August 2000 (fig. 1A). A strong seasonal pattern was not evident from monthly averages of TChl *a*, except for elevated concentrations of TChl *a* during the spring. Differences between months were significant (ANOVA, df = 11, F = 8.5, P < 0.01) and were driven by the months of March and April (data not shown).

Concentrations of taxon-specific pigments indicate that the phytoplankton community off the Scripps Pier consisted primarily of dinoflagellates, diatoms, prymnesiophyceae, "green" algae (predominantly prasinophyceae in the case of this study), pelagophyceae, cryptophyceae, eustigmatophyceae (only observed during September 1997), and the two cyanobacterial groups *Synechococcus* and *Prochlorococcus*. Dramatic differences in the abundance of the different taxonomic groups are evident (fig. 1 B-D). Dinoflagellates were responsible for the major blooms; their pigment biomass ranged from less than 0.01 μg Chl *a* $L^{-1}$ to ~10 μg Chl *a* $L^{-1}$ (fig. 1B). The biomass of other groups either varied with the seasons (e.g., chlorophyta, fig. 1C) or without distinct seasonal pattern (e.g., prymnesiophytes, fig. 1D). TChl *a* can also be partitioned into "larger autotrophs" (diatoms and dinoflagellates; fig. 1E) and "picoautotrophs" (prymnesiophytes, pelagophytes, cryptophytes, chlorophyta, eustigmatophyceae and cyanobacteria; fig. 1F). Temporal variability of TChl *a* was dominated by the larger autotrophs; these were responsible for 81% of the observed variability. The variability of picoautotroph abundance was small compared to that of the larger autotrophs. The pigment biomass of larger autotrophs differed significantly between months (ANOVA, df = 11, F = 9.6, P < 0.01), with monthly averages differing by a factor of 5. Blooms of larger autotrophs occurred primarily during March–June and during November. Picoautotroph pigment biomass also differed significantly between months (ANOVA, df = 11, F = 6.3, P < 0.01); however, monthly averages differed by only a factor of 2; results driven primarily by low values during June.

It is evident from the time series (fig. 1) that phytoplankton community structure varied with TChl *a*. To analyze this relationship in detail, the pigment biomass of different taxonomic groups was plotted against TChl *a* (fig. 2, see also Goericke 2002). Different types of patterns emerged: Variations of dinoflagellate biomass with TChl *a* were biphasic, as is evident from differences in slopes of point-clusters between 0.4 to 1.6 and 1.6 to 4 μg-TChl *a* $L^{-1}$. Dinoflagellates were the bloom taxon in this system, accounting for most of the phytoplankton biomass when TChl *a* was >2 μg $L^{-1}$ (fig. 2, left-hand

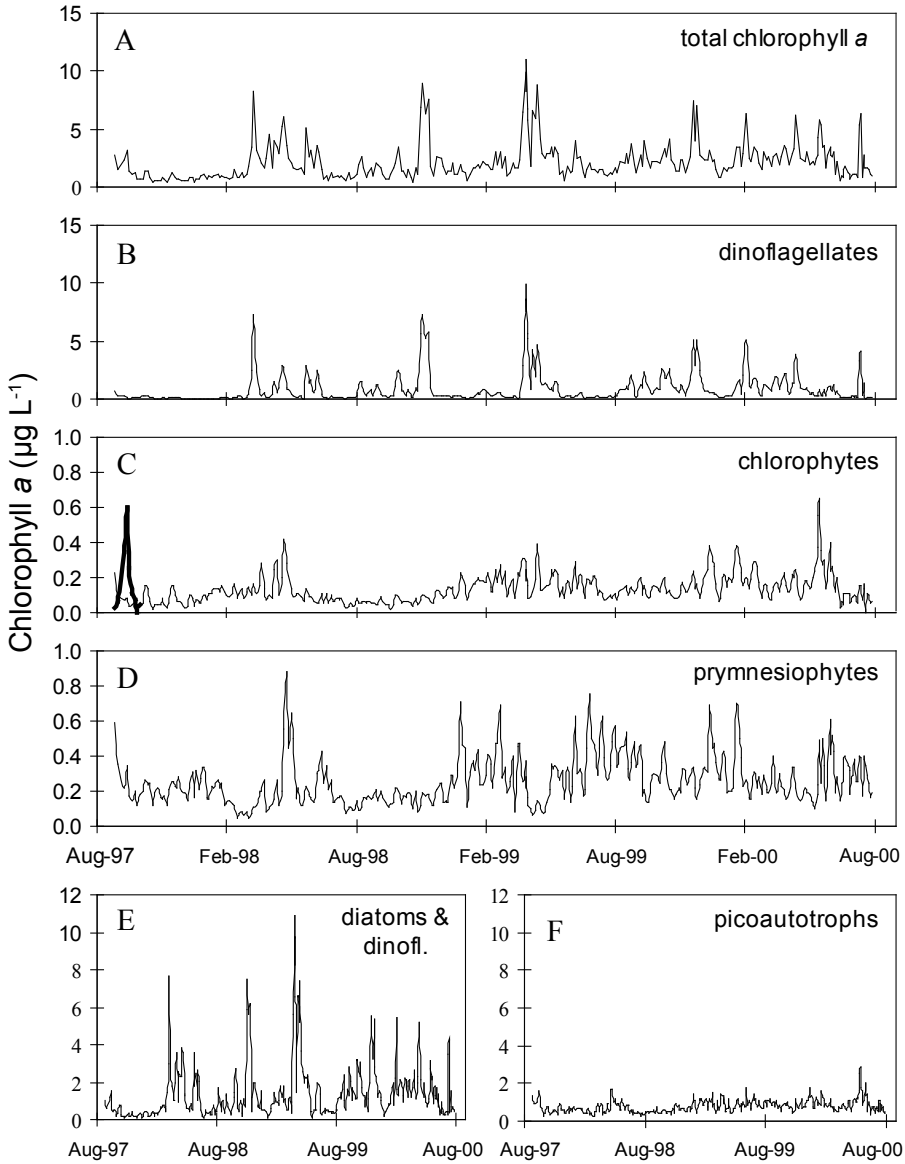


Figure 1. TChl *a* (A) and pigment biomass (Chl *a*) of dinoflagellates (B), chlorophyta (C), prymnesiophyceae (D), diatoms & dinoflagellates (E) and picoautotrophs (F) off the pier of the Scripps Institution of Oceanography (Scripps Pier). More pronounced dinoflagellate blooms or aggregations (TChl *a* > 100 µg $L^{-1}$) were observed in 1995, 1996 and 2001. The bold line in panel C likely represents eustigmatophyceae.

panel). The contribution of diatoms to TChl *a* increased linearly with TChl *a* and saturated at values of 1 to 1.5 µg Chl *a* $L^{-1}$ for TChl *a* of 4 to 10 µg $L^{-1}$. The pigment biomass of prymnesiophytes, pelagophytes, chlorophytes, and cryptophytes initially increased with TChl *a* and eventually leveled off at higher TChl *a*, reaching maximum values of 0.2 to 0.5 µg Chl *a* $L^{-1}$ (fig. 2). The biomass of *Synechococcus* increased only slightly with TChl *a*, saturating at concentrations of 0.15 to 0.2 µg $L^{-1}$, with possibly decreasing values when TChl *a* was larger than 4 µg $L^{-1}$. The biomass of *Prochlorococcus* appeared to decline with increasing TChl *a*; note, however, that measurements of Chl $a_2$ are unreliable when TChl *a* is larger than 4 µg $L^{-1}$ due to the interference of the large Chl $a_1$ peak with the more than 100 times smaller Chl $a_2$ peak. Overall, these data suggest that the biomass of the different groups of autotrophs, when plotted against TChl *a*, follows distinct and predictable patterns. Analyses carried out on one-year data batches yielded very similar results (data not shown), demonstrating that patterns were consistent from year to year.

To quantify these patterns, exponential functions were fit to the data. The functions used (table 1) took the following into account: 1. the potential presence of abundance thresholds (i.e., negligible contributions to total phytoplankton biomass below certain values of TChl *a*), 2. the asymptotic value reached when TChl *a* is large, 3. the biphasic patterns for dinoflagellates and 4. decreas-

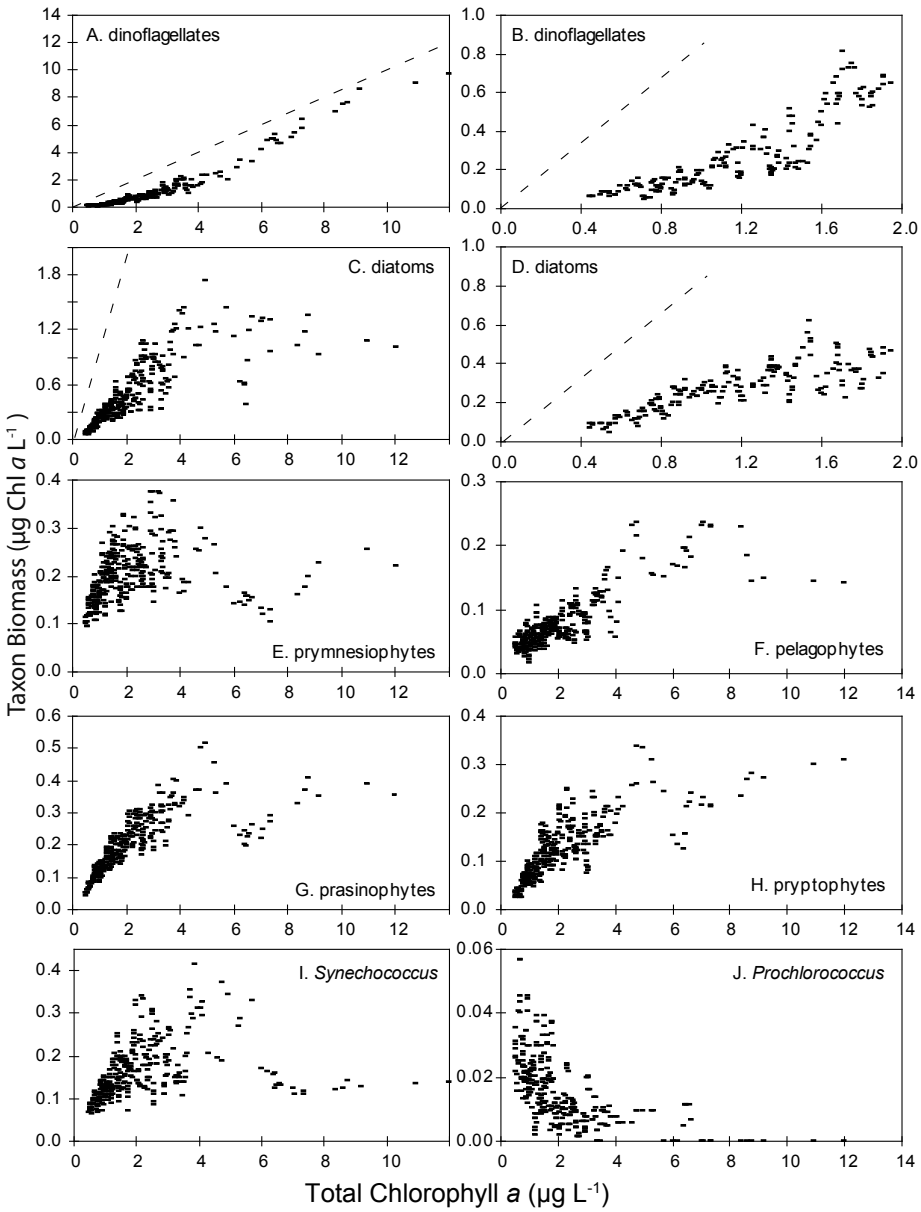


Figure 2. The pigment biomass of different groups of autotrophs off the Scripps Pier plotted against TChl *a*. The abundance of dinoflagellates and diatoms was plotted on entire TChl *a* scale (A, C) and on a reduced TChl *a* scale (B, D) to show variations of abundance at low TChl *a*. The dotted lines represent the 1:1 relationship. All data were subjected to 7-point smoothing to emphasize trends. Examples of unsmoothed data are shown in Figure 3 and 7.

ing pigment biomass for high values of TChl *a* in the case of *Synechococcus* and *Prochlorococcus*. The equations used are assumed to be descriptions of the data; no type of mechanism is implied by the use of any of these functions. These functions were fit to the raw data for the Scripps Pier and other environments (see below). Examples of curve fits are shown in Figure 3. The percent variance explained by these regressions (table 1) was high in most cases; up to 95% for some bloom taxa and on the average 42% for the other groups, with values of up to 75%. However, variance explained by the regressions was low for some groups, particularly *Synechococcus*; reflecting, for the most part, small variations of pigment biomass with TChl *a*. The three-parameter fits for diatoms and cryptophytes off the Scripps Pier suggest that abundance thresholds exist for these taxa, which is confirmed by data from other environments (see below). In the case of dinoflagellates the "threshold" parameter can not be interpreted as such due to the more complicated function used to describe biphasic abundance changes in the 0.4 to 2.0 µg $L^{-1}$ TChl *a* range. Asymptotic values of pigment biomass for the different taxonomic groups differed dramatically at the Scripps Pier, ranging from 0.8 µg Chl $L^{-1}$ for diatoms to 0.06 µg-Chl $L^{-1}$ for *Synechococcus*.

TABLE 1

**Parameter estimates for fits of exponential equations to plots of taxon-specific biomass vs. TChl *a* for the five environments studied. For *Prochlorococcus* the equation Biomass = $B_{max}$ (1-EXP(-$K_1$ (TChl *a* - Threshold)))-$K_2$ (TChl *a* - Threshold) EXP(-$K_3$ (TChl *a* - Threshold)$^2$)) was used. For all other groups Biomass = $B_{max}$ (1-EXP(-$K_1$ (TChl *a* - Threshold)))-$K_2$ (1-EXP (-$K_3$ (TChl *a* - Threshold))) was used. When threshold values for 3-parameter fits were less than 25% of the lowest value of TChl *a*, the threshold value was forced to be zero, which is indicated by 0 values in the table. $r^2$ designates the variance explained by the regressions. For 5-parameter fits values of "Threshold" are no longer interpretable as a threshold.**

Scripps Pier (0.4 - 11.0 µg Chl *a* L$^{-1}$)

| | dinoflagel. | diatoms | prymnesiop. | pelagop. | chlorop. | cryptop. | *Synechoc.* | *Prochloro.* |
|---|---|---|---|---|---|---|---|---|
| Threshold | –0.030 | 0.292 | 0 | 0 | 0.128 | 0 | 0.050 | 0.103 |
| $B_{max}$ | 90.76 | 0.802 | 0.262 | 0.173 | 0.195 | 0.242 | 0.204 | 0.015 |
| $K_1$ | 0.017 | 0.455 | 1.585 | 0.286 | 0.673 | 0.337 | 1.257 | 8.380 |
| $K_2$ | 6.412 | 0 | 0 | 0 | 0 | 0 | 0.131 | –0.090 |
| $K_3$ | 0.257 | 0 | 0 | 0 | 0 | 0 | 0.008 | 5.037 |
| $r^2$ (%) | 86 | 28 | 10 | 39 | 36 | 36 | 9 | 6 |

California Current System (0.03 - 10.6 µg Chl *a* L$^{-1}$)

| | dinoflagel. | diatoms | prymnesiop. | pelagop. | chlorop. | cryptop. | *Synechoc.* | *Prochloro.* |
|---|---|---|---|---|---|---|---|---|
| Threshold | 0.090 | 0.518 | 0.006 | 0.061 | 0.107 | 0.176 | 0 | 0.167 |
| $B_{max1}$ | 0.165 | 78.26 | 0.133 | 0.029 | 0.074 | 0.365 | 0.105 | 0.007 |
| $K_1$ | 0.555 | 0.013 | 2.587 | 7.062 | 1.314 | 0.274 | 3.149 | 6.508 |
| $B_{max2}$ | 0 | 0 | 0 | 0 | 0 | 0 | 0.089 | –0.324 |
| $K_2$ | 0 | 0 | 0 | 0 | 0 | 0 | 1.562 | 25.29 |
| $r^2$ (%) | 26 | 95 | 46 | 21 | 64 | 75 | 26 | 51 |

Southern Indian Ocean (0.02 - 1.44 µg Chl *a* L$^{-1}$)

| | dinoflagel. | diatoms | prymnesiop. | pelagop. | chlorop. | cryptop. | cyanobac. | *Prochloro.* |
|---|---|---|---|---|---|---|---|---|
| Threshold | 0.041 | 0.027 | 0 | 0.015 | 0.063 | 0 | n.d. | 0 |
| $B_{max1}$ | 1.389 | 54.44 | 0.17 | 0.180 | 0.307 | 0.222 | n.d. | 1.302 |
| $K_1$ | 0.068 | 0.008 | 1.070 | 0.189 | 1.879 | 0.172 | n.d. | 7.408 |
| $B_{max2}$ | 0 | 0 | 0 | 0 | 0 | 0 | n.d. | 1.298 |
| $K_2$ | 0 | 0 | 0 | 0 | 0 | 0 | n.d. | 6.140 |
| $r^2$ (%) | 73 | 69 | 66 | 73 | 84 | — | — | — |

Arabian Sea (0.14 - 1.88 µg Chl *a* L$^{-1}$)

| | dinoflagel. | diatoms | prymnesiop. | pelagop. | chlorop. | cryptop. | *Synechoc.* | *Prochloro.* |
|---|---|---|---|---|---|---|---|---|
| Threshold | 0 | 0.296 | 0.025 | 0.071 | 0.084 | 0.187 | 0 | 0.010 |
| $B_{max1}$ | 0.034 | 54.07 | 0.368 | 0.048 | 0.104 | 0.622 | 0.034 | 1.289 |
| $K_1$ | 1.451 | 0.009 | 2.29 | 5.694 | 1.399 | 0.115 | 109 | 12.63 |
| $B_{max2}$ | 0 | 0 | 0 | 0 | 0 | 0 | 0 | 1.286 |
| $K_2$ | 0 | 0 | 0 | 0 | 0 | 0 | 0 | 9.533 |
| $r^2$ (%) | 39 | 68 | 57 | 23 | 25 | 55 | 0 | 45 |

Sargasso Sea - (0.01 - 0.54 µg Chl *a* L$^{-1}$)

| | dinoflagel. | diatoms | prymnesiop. | pelagop. | chlorop. | cryptop. | cyanobac. | *Prochloro.* |
|---|---|---|---|---|---|---|---|---|
| Threshold | 0.026 | 0 | 0 | 0.016 | 0.146 | n.d. | 0 | n.d. |
| $B_{max1}$ | 0.004 | 0.016 | 2.288 | 0.659 | 0.066 | n.d. | 0.042 | n.d. |
| $K_1$ | 144.4 | 5.121 | 0.255 | 0.456 | 1.444 | n.d. | 2.356 | n.d. |
| $r^2$ (%) | 54 | 29 | 96 | 90 | 62 | — | 19 | — |

***California Current System.*** To test the generality of these patterns, similar analyses were carried out on pigment data from the mixed layer of the California Current system at stations 5 to ~700 km off the coast of Southern California. Concentrations of TChl *a* usually declined from values of up to 10 µg L$^{-1}$ in eutrophic coastal regions to values of <0.1 µg L$^{-1}$ in oligotrophic offshore regions. The biomass of diatoms, dinoflagellates, cryptophytes and chlorophytes (fig. 4) was negligible when TChl *a* fell below threshold values that ranged from 0.1 to 0.5 µg L$^{-1}$. No such thresholds were observed for prymnesiophytes, pelagophytes, *Synechococcus* and *Prochlorococcus*. Diatoms were the bloom taxon in this system and dominated phytoplankton biomass when TChl *a* was high (fig. 4). Dinoflagellate biomass in the CCS reached maxium values of less than 1 µg Chl *a* L$^{-1}$. Chlorophyte and cryptophyte biomass (fig. 4) reached maxium values of ~0.1 and 0.2 µg Chl a L$^{-1}$,

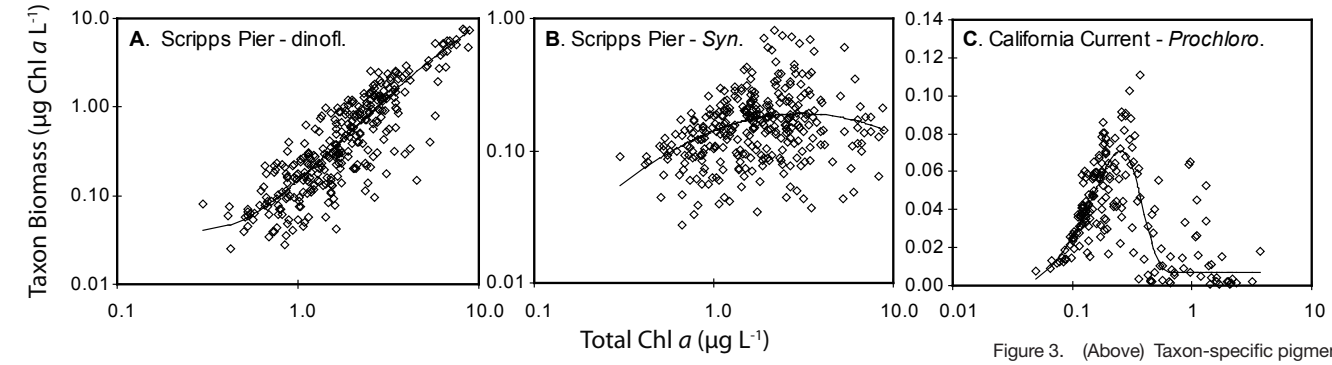


Figure 3. (Above) Taxon-specific pigment biomass plotted against TChl *a* (discrete symbols) and fits of exponential functions (solid lines) to these data for dinoflagellates (A) and *Synechococcus* (B) off the Scripps Pier and *Prochlorococcus* in the California Current system (C). Parameter values for the curves are given in Table 1.

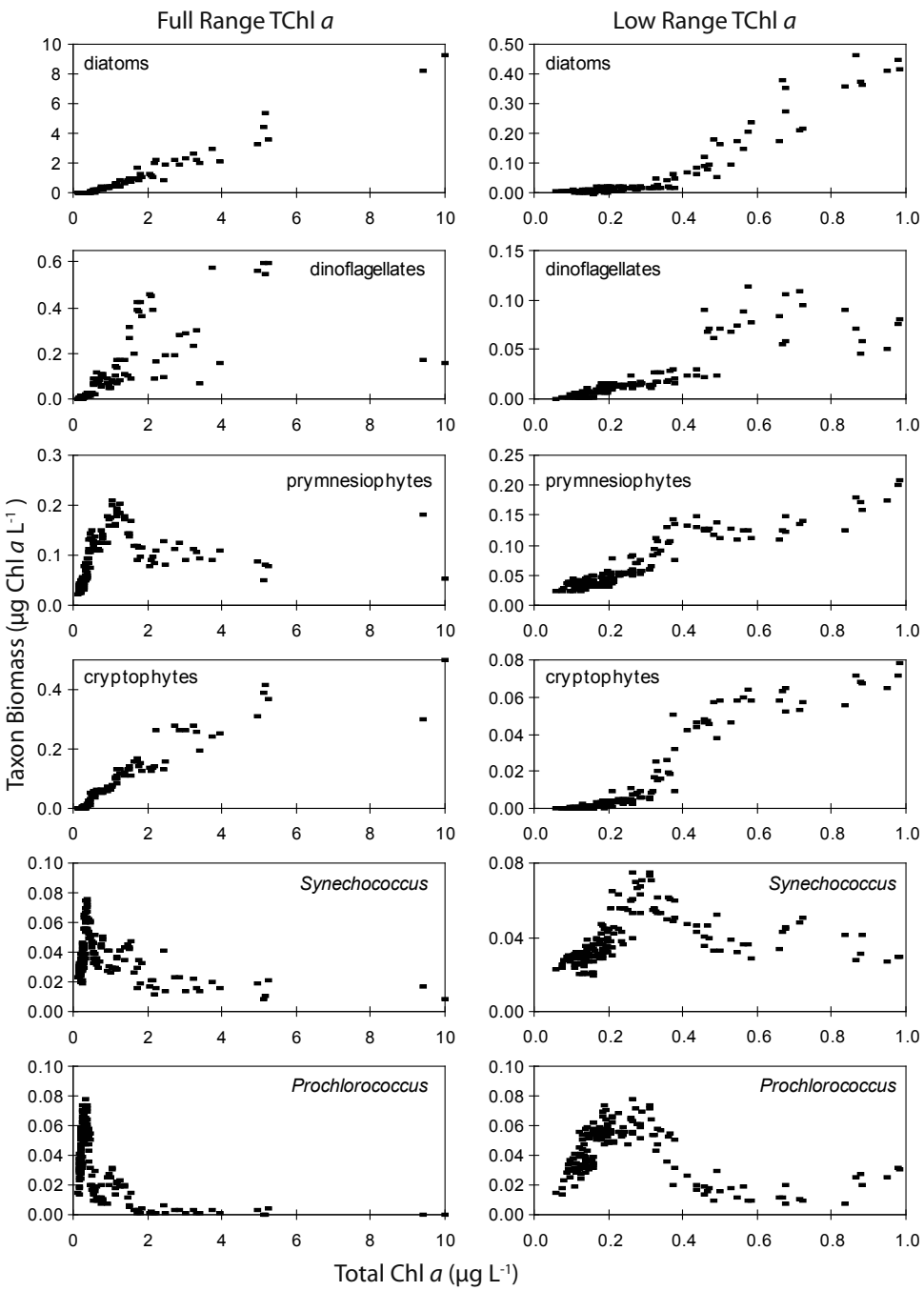


Figure 4. The pigment biomass of selected algal taxa plotted against TChl *a* for the California Current system. All data were subjected to 7-point smoothing. Unsmoothed data for *Prochlorococcus* are shown in Figure 3C. Plots in the left-hand column are for the whole range of TChl *a* values and plots in the right-hand column are for TChl *a* < 1 µg $L^{-1}$. Note the different scales of the abscissae in the left- and right-hand columns.

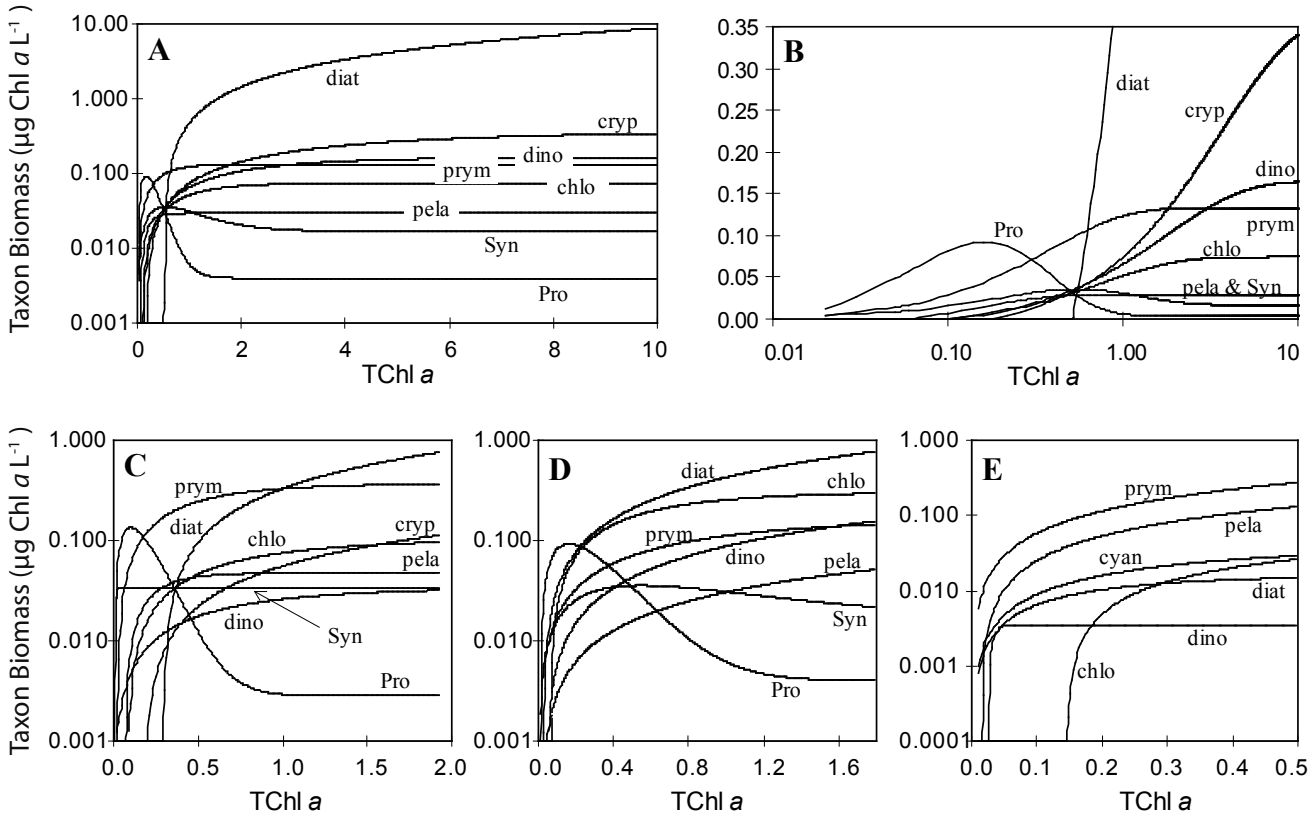


Figure 5. Regressions of pigment biomass of different taxa against TChl *a* for the California Current system (A, B), the Arabian Sea (C), the Southern Indian Ocean (D), and the Sargasso Sea (E). Taxa are diatoms (diat), *Prochlorococcus* (Pro), cryptophytes (cryp), dinoflagellates (dino), prymnesiophytes (prym), chlorophytes (chlo), pelagophytes (pela), *Synechococcus* (Syn) and cyanobacteria (cyan, in case it was not possible to differentiate between Syn and Pro). Note the change of scales of axes between Figure 5A and B. Equations and parameter values for these regressions are given in Table 1.

respectively, when TChl *a* reached values of 3–5 µg $L^{-1}$. The contributions of *Synechococcus* to TChl *a* increased linearly with TChl *a* up to values of 0.3 µg $L^{-1}$ and decreased above this value (fig. 4). Variations of *Prochlorococcus* biomass with TChl *a* were very similar to variations of *Synechococcus* biomass (fig. 4). Nonlinear regressions of taxon-pigment biomass against TChl *a* accounted for a large fraction of the total variability for most groups (fig. 5A, B; table 1). The predicted abundance of different taxa as a function of TChl *a* is shown in Figure 5 A and B for the California Current system, which illustrate changes of the phytoplankton community as TChl *a* increases. The implication of the plots is that the changes are driven by increasing nutrient loading or nutrient content, sensu Thingstad (1998), of the system. However, observed changes could also be due to geographical differences within the study domain.

***Enrichment Experiments.*** To differentiate between these two possible explanations of the field data, the response of phytoplankton community structure to nutrient enrichments was studied. In October 1996 six experiments were performed in the California Current system with water collected from the mixed layer in regions with undetectable and detectable levels of macronutrients. Moderate phytoplankton blooms were always observed in incubation bottles enriched with ammonium and nitrate, or in samples naturally enriched with nutrients. No blooms were observed in low-nutrient controls or in phosphate enrichments (data to be presented elsewhere). Blooms in incubation bottles were dominated in all cases by diatoms; the biomass of other groups of algae also increased in response to nutrient enrichments but never as rapidly as observed for diatoms. Diatoms did not contribute significantly to TChl *a* when TChl *a* was less than 0.5 µg $L^{-1}$ (fig. 6). This threshold value is similar to values observed in situ (cf. fig. 4). The biomass of all other groups of algae reached maximum values as TChl *a* increased, ranging from 0.03 µg Chl *a* $L^{-1}$ for dinoflagellates to 0.3 µg Chl $L^{-1}$ for prymnesiophytes. In most cases there was a good correspondence, qualitatively, between variations of taxon-specific pigment biomass with TChl *a* for experiments (discrete symbols in fig. 6) and those observed in situ (lines in fig. 6 derived from fits to data shown in fig. 4). The exceptions were cyanobacteria, whose biomass did not decrease as TChl *a* increased, unlike pattern observed in situ (fig. 4).

***Other Environments.*** To explore if biomass distribu-

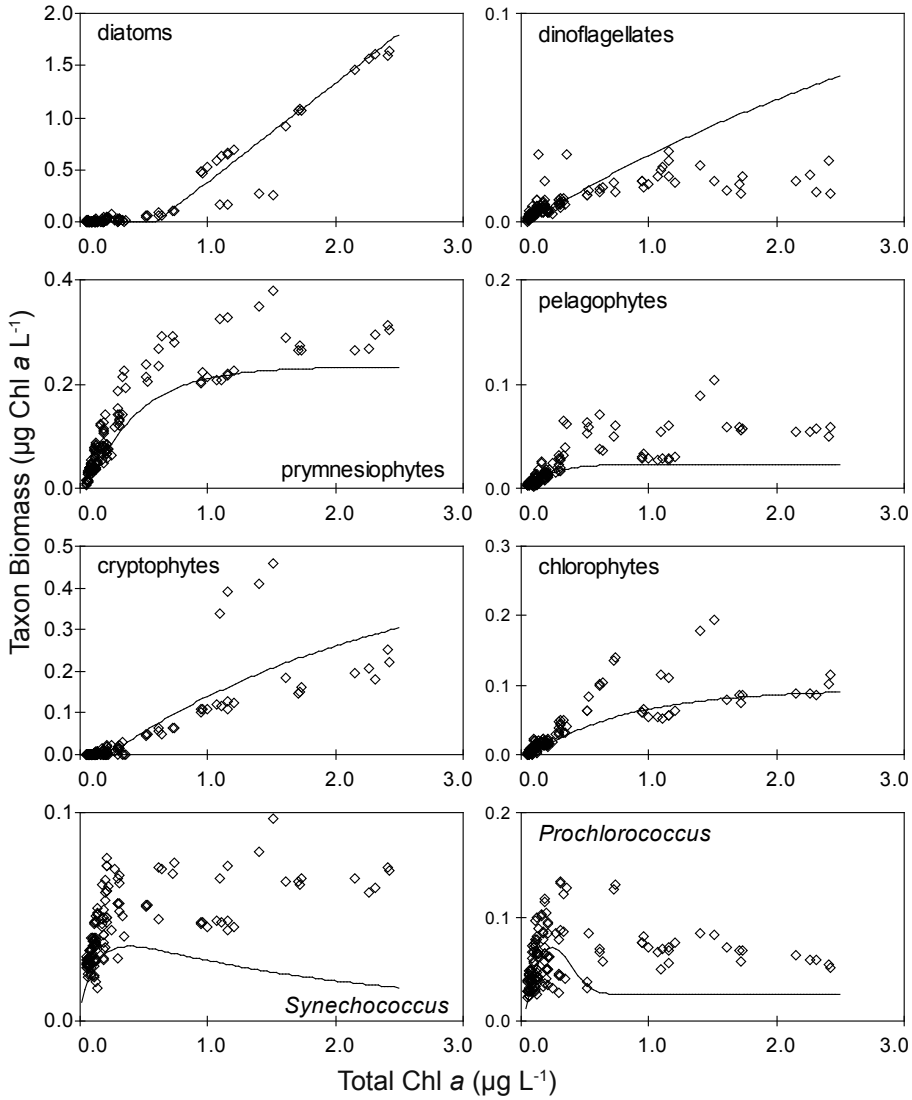


Figure 6. The pigment biomass of selected algal taxa plotted against TChl *a* for nutrient enrichment experiments performed in October 1996 in the California Current system (open diamonds). All experimental time points, i.e., t=0 to t=72 hours, were plotted. Lines are regressions of in situ data from the same time period (samples from the mixed layer collected during CalCOFI cruise 9610); i.e., these are not regressions derived from data points shown here. TChl *a* at time zero ranged from 0.08 to 0.85 µg $L^{-1}$.

tions in other environments are similar to those found off Southern California, mixed-layer-pigment data sets from the Southern Indian Ocean, the Sargasso Sea and the monsoonal Arabian Sea were analyzed. The pigment biomass of different taxa was determined for these environments (for the Arabian Sea see fig. 8 of Goericke 2002) and data were regressed against TChl *a* (table 1). The observed patterns were qualitatively similar among the different environments, as illustrated in Figure 5 for the complete data sets and in Figure 7 for prymnesiophytes and chlorophytes from different environments. This similarity is also reflected in the parameter values derived from the regressions (table 1). For example, asymptotic values of pelagophyte biomass ($B_{max}$) ranged from about 0.05 to 0.2 µg Chl $L^{-1}$, in those environments where it could be estimated accurately; a very narrow range considering that maximal values of TChl *a* ranged from 0.5 to 10 µg $L^{-1}$. Similarly, values of chlorophyte abundance thresholds and $B_{max}$ (fig. 7) were 0.11 $\pm$ 0.03 and 0.15 $\pm$ 0.10 µg Chl $L^{-1}$, respectively, in five different environments. In some cases parameter values differ dramatically between environments for any one group. Examples are parameters describing diatom and dinoflagellate distributions.

## DISCUSSION

***Describing Phytoplankton Community Structure.*** The structure of the phytoplankton community was explored using taxonomic units as defined by taxon-specific pigments. The data presented here and physiological data

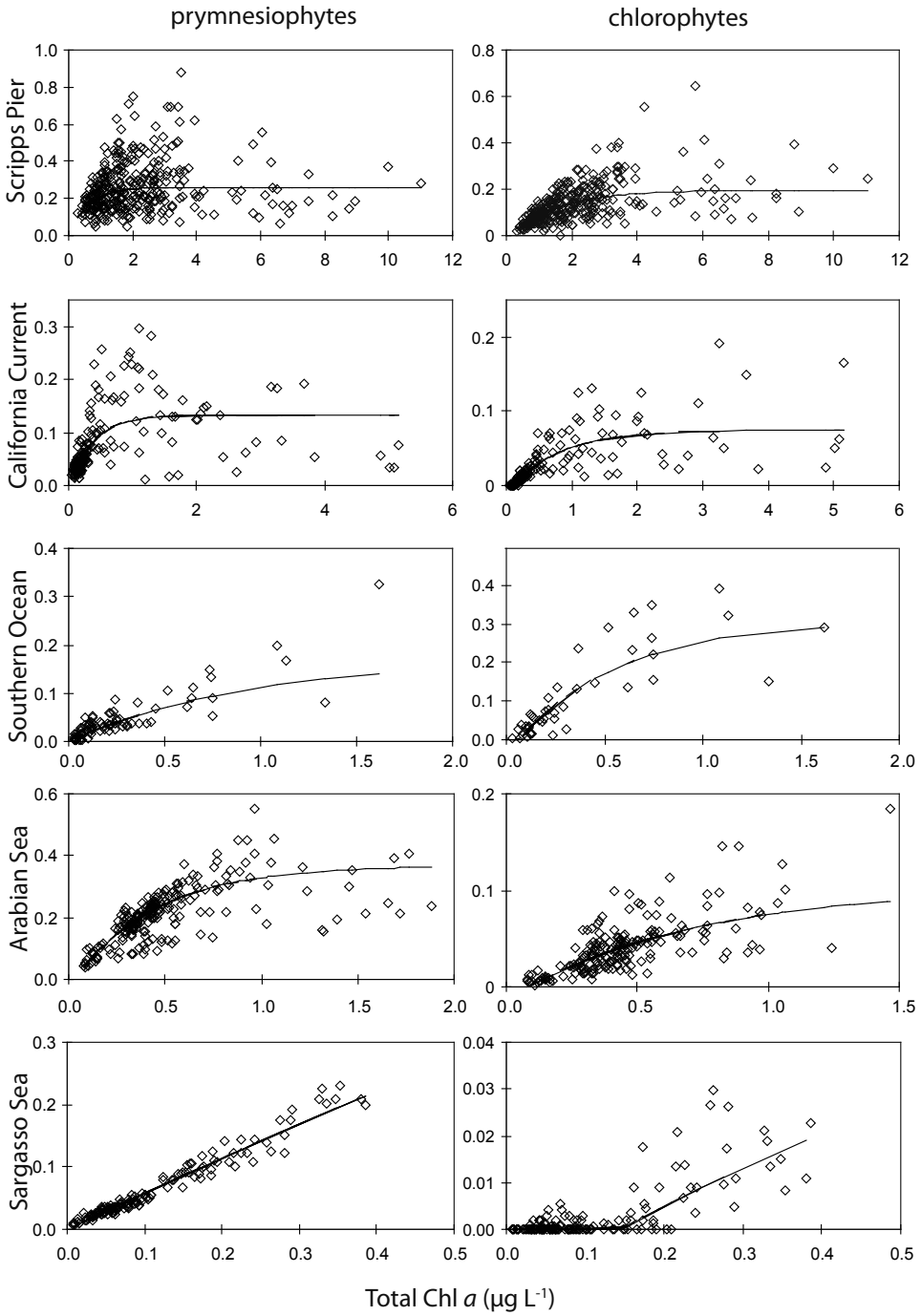


Figure 7. Prymnesiophyte and chlorophyte pigment biomass plotted against TChl *a* for the Scripps Pier, the California Current system, the Southern Indian Ocean, the monsoonal Arabian Sea (open ocean stations only) and the Sargasso Sea (BATS Station). Data were not smoothed.

presented by others (e.g., Claustre 1994; Latasa et al. 1997; Goericke 1998; Brown et al. 2002; Goericke 2002) demonstrate that these broad pigment-defined taxonomic categories are functionally and ecologically distinct units. The abundance of these groups off the Scripps Pier, in the California Current system, the Arabian Sea, the Sargasso Sea and the Southern Indian Ocean (Goericke 2002, this study) varied predictably as a function of TChl *a* and varied coherently along transects more than 1000 km long. Distributional patterns differed significantly among groups. In the Arabian Sea growth rates of these groups, measured using the pigment labeling method, varied predictably as a function of a proxy for the availability of inorganic nitrogen and also differed significantly among groups (Goericke 2002). Indeed, these data show that categories delineated by

taxon-specific pigments are one solution to the aggregation problem (O'neill et al. 1986) which has baffled phytoplankton ecologists for the last century; i.e., How can a phytoplankton community be partitioned into functionally relevant aggregates that are more amenable to study than the 100s of species it consist of?

The interpretation of patterns observed in the field is not straightforward since TChl *a* varied in many environments as a function of latitude and/or distance from shore and, associated with that, temperature. The observed distributions could simply reflect the presence of different phytoplankton communities in different regions of the study domain or the advection of different water masses with differing phytoplankton communities into specific regions. However, an underlying assumption of the approach is that observed changes within any study domain are similar to changes that would occur if an enrichment of the system occurred at that point. The enrichment experiments that were performed in the California Current system and the grow-out experiments performed in the Arabian Sea (Goericke 2002) are tests of this assumption. Indeed, changes of phytoplankton community structure with TChl *a* observed over the course of these experiments in the California Current system (fig. 6) and the Arabian Sea (fig. 10 of Goericke 2002) were qualitatively and, for the most part, quantitatively very similar to observations in the field. Thus, results from these experiments demonstrate that differences in phytoplankton community structure observed over the whole study domain can also occur at any one point of the study domain when an enrichment of the system occurs.

***What are the Patterns—Are there Rules?*** The variability of autotroph biomass off the Scripps Pier was primarily due to blooms of dinoflagellates and to some extent diatoms, i.e., the larger autotrophs that contributed 81% to the variability of TChl *a* over time (fig. 1E). Their contributions to TChl *a* ranged from 0.04 to 10 μg $L^{-1}$, in strong contrast to the contributions of prymnesiophytes, pelagophytes, chlorophytes, cryptophytes and cyanobacteria, i.e., the "picoplankters" (fig. 1F), whose contributions ranged from 0.2 to 1.8 μg Chl a $L^{-1}$. Seasonal variability off the Scripps Pier is similarly dominated by larger autotrophs; while seasonal variation of picoautotroph biomass is small. A striking aspect of the data from the Scripps Pier is the absence of any obvious correlation between the bloom periods of the larger autotrophs and the abundance of picoautotrophs. Indeed, the abundance of picoautotrophs is not significantly related to the abundance of larger autotrophs for TChl *a* > 1 μg $L^{-1}$. These results do not imply that some picoautotrophs do not go through bloom periods. At times *Synechococcus* biomass increased more than 5-fold over average values; eustigmatophyceae (fig. 1C, Sept. 1997) are another good example. However, these blooms of picoautotrophs were not large contributors to the variability of total biomass.

Results from the California Current system, the Arabian Sea and the Southern Indian Ocean are strikingly similar: The variability of phytoplankton biomass in these oceanic regions was dominated by diatoms while the biomass of all other groups saturated at specific levels, often significantly lower than values of TChl *a*. Malone (1971), Mullin (1998; 2000) and Anderson et al. (2008) similarly noted that variations of pigment biomass in the California Current were primarily driven by larger size classes. Claustre (1994), based on the analysis of pigment samples from the North Atlantic and the Mediterranean Sea, also found that the variability of pigment biomass was dominated by diatoms and dinoflagellates. These results support the rule that picoautotrophs are the ever-present lawn of the ocean, on which the occasional, large tree, the diatom or dinoflagellate bloom, is found that supports orders of magnitude higher levels of autotroph biomass (Chisholm 1992; Li 2002; Goericke 2011). This rule implies that the variability of autotroph biomass in the ocean is dominated by larger autotrophs, diatoms in most cases. It is likely that this rule also applies to other environments that are similar to the ones studied. But this rule is clearly not universally valid. For example, blooms of the picoautotroph *Chrysochromolina* sp. have been observed off the west coast of Sweden and blooms of the prymnesiophytes *Pheocystis pouchetii* and *Emiliania huxleyi* are known to occur in many regions of the world's ocean. These exceptions do not invalidate the proposed rules, as rules are only persistent patterns with possible or known exceptions; rules without possible exceptions are laws. The existence of such rules is important for our understanding of the ocean, as their existence implies that the mechanisms that control or generate these patterns are the same, or at least similar, in different environments.

Detailed size-fractionation experiments performed in the Mediterranean Sea suggested that the amount of TChl *a* in the <1, <3, and <10 μm size fractions have upper bounds of 0.5, 1, and 2 μg $L^{-1}$, and that Chl *a* is added to the system by first completing the "quotas" of the smallest size class before filling the next one (Raimbault et al. 1988). Thus, contributions of different size classes to TChl *a* are thought to display saturation patterns with differing maximum contributions to TChl *a*. Since specific phytoplankton taxa are often associated with distinct size classes (Chisholm 1992), similar saturation patterns were expected for plots of the abundance of different taxa against TChl *a*, which was indeed observed (fig. 2, 4 and Goericke 2002). Common to all environments studied so far is the presence of a bloom taxon—dinoflagellates off the Scripps Pier

and diatoms in the California Current system, the Arabian Sea and the Southern Indian Ocean. The Arabian Sea was unusual since blooms did not occur offshore in spite of high growth rates and replete nutrients. However, diatom blooms were observed in incubation bottles and close to the coast, suggesting that diatom abundance offshore was controlled by grazers, i.e., top-down forces (Goericke 2002). The abundance of other taxa in all these environments covaried with TChl *a* at low values, but leveled off to constant values as TChl *a* increased to values larger than 1 to 4 μg $L^{-1}$. The average maximum biomass reached by some of the taxa, e.g., cryptophytes, pelagophytes, and chlorophytes, was surprisingly similar in most environments (table 1). Similarly, some of the taxa consistently had abundance thresholds, which also were similar in the different environments; examples are chlorophytes and cryptophytes (table 1).

Whereas distributions of eukaryotes were, for the most part, characterized by simple saturating functions with or without abundance thresholds, variations of *Synechococcus*, and in particular *Prochlorococcus* biomass with TChl *a* were characterized by initial increases, maximum biomass at low levels of TChl *a*, followed by decreases as TChl *a* reached high values. In the Arabian Sea this decrease was only in part related to temperature, since a similar decrease was observed during grow-out experiments at constant temperature (Goericke 2002). High levels of TChl *a* in the California Current system were also related to low temperatures, likely accounting for some of the observed decrease of *Prochlorococcus* biomass. However, such a decrease, albeit not as strong, was observed as TChl *a* increased during nutrient enrichment experiments, suggesting that it is also driven by community processes. The decrease of *Synechococcus* biomass for high values of TChl *a* was less pronounced, but still evident, off the Scripps Pier and in the California Current system. Claustre (1994) observed similar patterns for pigments likely derived from cyanobacteria in the North Atlantic and the Mediterranean.

***Predicting the Patterns.*** Time series of taxon-specific pigment biomass (e.g., fig. 1) reflect the short-term variability of phytoplankton biomass, which is likely driven by varying rates of nutrient-autotroph and autotroph-heterotroph interactions. Understanding such patterns is possible in principle; however, making predictions of these over large spatial or temporal scales is virtually impossible. The problem is quite similar to that faced by meteorologists: Weather can only be predicted over short temporal scales. However, climate, which is weather expected on the average, can accurately be specified for particular times of the year or for specific conditions, such as an El Niño, as long as historical weather records are available. The approach proposed here is quite similar: It is suggested that relationships between taxon-specific biomass and TChl *a* are used to predict the composition of the community for any value of TChl *a*. Or rephrased, it is proposed that such relationships be used to characterize the "ecological climate", realizing that such relationships can not be used to predict the "ecological weather".

The quantitative relationships derived here (e.g., fig. 6) will allow us more accurate descriptions, predictions and explanations. For example, studies off Bermuda noted that spring phytoplankton blooms were not dominated by diatoms (Goericke 1998; Steinberg et al. 2001), even though this was the case during the late 1950s (Hulburt et al. 1960; Menzel and Ryther 1960). This could be interpreted as a change of the phytoplankton community over the last few decades. However, when diatom blooms were observed during the late 1950s, surface layer Chl *a* was at least 1 μg $L^{-1}$; recently only values of up to 0.5 μg Chl *a* $L^{-1}$ were observed (Goericke 1998; Steinberg et al. 2001). A comparison of the Sargasso Sea biomass plot (fig. 5E) with those from other regions (e.g., fig. 5A) suggests that values of TChl *a* in the Sargasso Sea never reached likely threshold levels for diatoms (~0.5 μg Chl *a* $L^{-1}$) to contribute significantly to TChl *a*. Observations made in eddies off Bermuda (Ewart et al. 2008) and in other oligotrophic environments (Brown et al. 2002) corroborate this interpretation.

Some of the observed distributions of non-bloom taxa are strongly related to TChl *a*; regressions of pigment biomass for some taxa against TChl *a* explain up to 70% of the variance in the data sets. It is straightforward using these relationships to predict the abundance of those groups of autotrophs to TChl *a* with a high degree of confidence. Variance explained by the regressions is very low for other taxa though, particularly *Synechococcus*. This result, however, does not imply that the biomass of these groups cannot be predicted; it only implies that the abundance of these groups is relatively invariant in these environments. Powerful predictions can still be derived from such relationships, as is the case for the monsoonal Arabian Sea were the expected pigment biomass of *Synechococcus* is 0.04 μg Chl $L^{-1}$ with a standard error of 0.02 μg Chl $L^{-1}$ for TChl *a* ranging from 0.1 to 1.8 μg $L^{-1}$.

The data presented here constitute a very simple means to predict phytoplankton community structure from TChl *a*. The relationships between taxon-specific biomass and TChl *a* can be described using functions with 2 to 5 free parameters. Considering that TChl *a* can be remotely sensed, or is a standard product of coupled biological-physical models, such relationships may be the simplest means to incorporate phytoplankton community structure into biophysical models that cannot be burdened with detailed descriptions of the interactions between different taxa of autotrophs and different classes

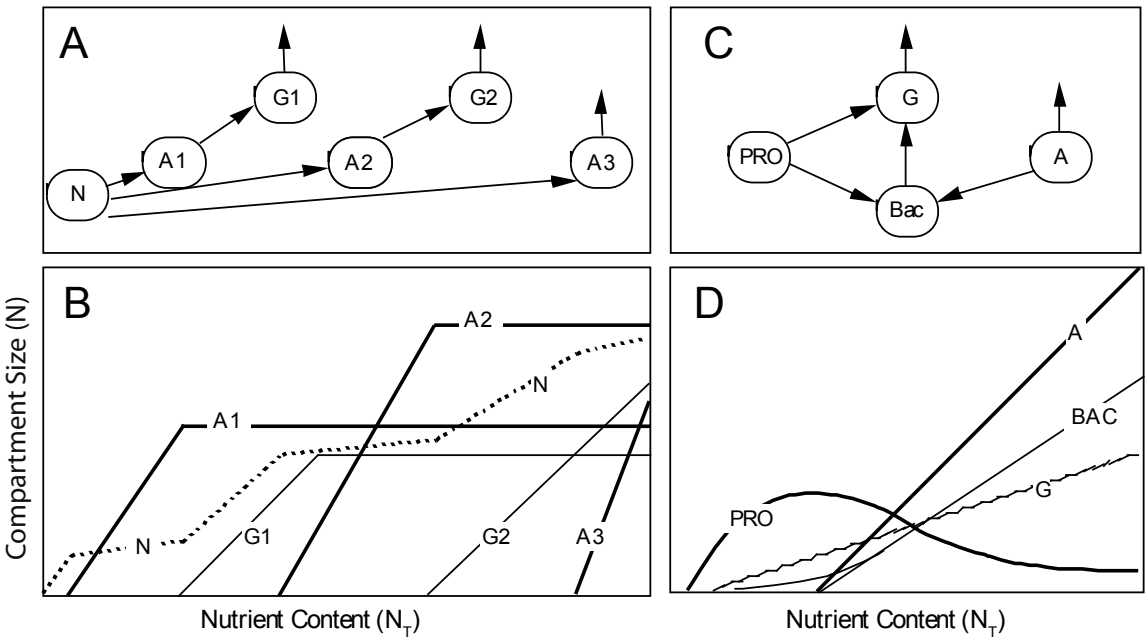


Figure 8. Food web diagrams and predicted biomass variations as a function of a system's nutrient content ($N_T$). A. Food web consisting of one nutrient pool (N), three autotrophs (A1, A2, A3) and two grazers (G1, G2). B. Variations of predicted nutrient concentrations and autotroph and grazer biomass as a function of $N_T$ for the system shown in A (adapted from Thingstad, 1998). C. A food web showing interactions between *Prochlorococcus* (PRO), one grazer (G), heterotrophic bacteria (BAC) and other autotrophs (A). D. Biomass variations of autotrophs (PRO, A), heterotrophic bacteria (BAC) and a grazer (G) as a function of nutrient content for the system shown in C.

of grazers. Clearly, such models would not contribute to our understanding of the controls of phytoplankton community structure, but these models could contribute to our understanding of the effects of phytoplankton community structure on carbon cycling. Critical to such approaches to modeling is a good understanding of the limitations of such data sets. For example, the different distributions observed off Southern California in the nearshore and the California Current system suggest that nearshore communities differ fundamentally from coastal oceanic communities (see also Goericke 2002). Clearly, it is necessary to characterize nearshore, coastal and oceanic phytoplankton communities in greater detail. A second example is distributions for cyanobacteria that suggest that temperature may exert important secondary effects on phytoplankton community structure. Taking this into account might allow us to better describe and predict of variations of phytoplankton community structure in the ocean. Unfortunately, the data in hand do not allow us to do this since temperature and phytoplankton biomass are too strongly related (data not shown).

***What are the Mechanisms?*** Marine pelagic communities are likely never at steady state, due to continuously varying physical forcing. Thus it is practically impossible to predict the state of the community accurately at any point of time or space. Instead one can attempt to understand and predict the average state of pelagic communities. Plotting the abundance of different taxa against TChl *a* and calculating the average distributions (fig. 5) conveys such an average state of the system. A conceptual model that allows us to understand the average state of pelagic communities has been proposed by Thingstad (1998). Thingstad's models are centered on the control that the "nutrient content" of the photic zone exerts on the size structure of the phytoplankton community. In this context "nutrient" refers to that element that limits total biomass in the system, or at least the biomass of most compartments of the system. The nutrient content ($N_T$) of the system is the sum of the concentrations of this element in all compartments of the system. Increasing the flux of this *critical* nutrient into the photic zone is expected to increase total standing stock of the organisms.

For this study, TChl *a* is used as an index of phytoplankton biomass. Relationships between TChl *a* and phytoplankton biomass are variable but predictable (Geider et al. 1996; Goericke and Montoya 1998). Phytoplankton biomass can be assumed to covary roughly within any one environment with the biomass of other trophic levels (Sheldon et al. 1977; Sprules and Munawar 1986). Thus, it is possible to view TChl *a* in this context as a proxy for $N_T$ and to interpret varying TChl *a*, at least on the average, as varying fluxes of the critical nutrient into the system. Even though it can and should not be assumed that the relationship between TChl *a* and $N_T$ is linear, it is quite likely that the relationship between the two parameters is governed by a monotonically increasing function.

Thingstad's conceptual model (1998) predicts biomass variations of different size classes of autotrophs with increasing $N_T$ that are strikingly similar to biomass variations of different taxa with TChl *a* (cf. fig. 5). Thingstad assumes that the system is at steady state and discusses changes of the community as $N_T$ increases. Thus, the focus of Thingstad's analysis is not the transients that result when fluxes of a nutrient into a system are increased; rather it is how the steady state of an ideal system changes as a function of $N_T$. When $N_T$ is zero, organisms, by definition, do not exist. When $N_T$ increases, the first organism capable of growing must be that autotroph (A1) that has the highest affinity for the critical nutrient (N). This will be the smallest autotroph capable of living in the system (fig. 8A, B). Data presented here and those discussed by others (e.g., Campbell et al. 1994) support this prediction since *Prochlorococcus*, the smallest known photoautotroph (Chisholm et al. 1992), dominates phytoplankton abundance when TChl *a* is extremely low (fig. 5). Further increasing $N_T$ increases the biomass of the autotroph A1.

The presence of A1 opens a niche for a grazer (G1) capable of feeding on A1. As $N_T$ increases the biomass of A1 and G1 will increase as well. Thingstad postulated that the dynamics of the predator-prey pair will increasingly be decoupled from the availability of N; i.e., eventually reaching a stable equilibrium or exhibiting stable limit cycles (e.g., May 1981). At this point the biomass of A1 and G1 will be independent of $N_T$ and will remain constant, at least when averaged over appropriate time periods. Thus, the predicted dependence of A1 on $N_T$ is linear for low values of $N_T$, but eventually levels off and reaches a constant value at high values of $N_T$. The predicted patterns (fig. 8B) are similar to variations of observed taxon-specific biomass with TChl *a* (fig. 5). A corollary of the conceptual model is that autotroph division rates will be maximal, i.e. unconstrained by the availability of inorganic nutrients, once the biomass no longer increases with $N_T$. This implies that plots of biomass variations (e.g., fig. 2) could be used to determine when groups of autotrophs are expected to grow at rates close to their physiological maxima; a hypothesis that still has to be tested.

As the biomass of A1 and G1 becomes increasingly independent of $N_T$, further increases of $N_T$ opens a niche for a second, larger autotroph (A2). The abundance of A2, when plotted against $N_T$, will display a threshold similar to those observed for chlorophytes, cryptophytes and diatoms in the California Current system (fig. 4). The increase of A2 opens a niche for a second grazer G2. As $N_T$ further increases the biomass of A2 and G2, they will reach constant levels when their rates of growth and loss are, on the average, balanced. Further increases of $N_T$ will open a niche for a third, yet larger, autotroph A3, etc. The predicted variations of A1, A2 and A3 abundance with $N_T$ (fig. 8B) are very similar to field data presented above (fig. 5). The progressive waves of autotrophs and grazers will come to an end once a mismatch arises between the response time scales of the autotrophs to increasing levels of nutrients and the response time scales of the grazers to increasing biomass of larger autotrophs (e.g., Franks 2001). This state is usually reached once the grazers are crustaceans. Whereas maximum growth rates of protozoa overlap those of their prey (e.g., Fenchel and Finlay 1983), maximum growth rates of crustacean grazers are roughly one order of magnitude less than that of their prey (Banse 1982). Thus, blooms of large autotrophs are expected once a mismatch has been established between the response time scales of the prey and predator.

The characteristic feature of the model is, as noted by Thingstad (1998), that strong top-down forces limit the biomass of smaller autotrophs and open up niches for larger autotrophs. Even though total phytoplankton biomass may be limited by the availability of a critical nutrient, i.e., by bottom-up effects, the biomass of most individual taxa is controlled by grazers, i.e., top-down forces, except for the largest taxon that form blooms. Clearly, there are differences between the predictions of the idealized model of Thingstad (1998) and the field data. The field data do not show a staggered succession of autotrophs; rather, new taxa of autotrophs appear before the biomass of those taxa, that are already present, has saturated. This is no surprise; the above predictions were only based on the presence of a single nutrient and no interactions between herbivores or grazing of herbivores on multiple autotroph taxa were considered. It is quite conceivable that other environmental factors and additional biological interactions exert secondary effects, which open up niches for other autotrophs. Even though these differences exist between the predicted and observed patterns, the predictive capabilities of the conceptual model are surprising once the similarities of patterns shown in Figure 5 and Figure 8B are considered.

The only pattern that is not predicted by the model is the decline of the biomass of *Prochlorococcus* for large values of TChl *a*. It was discussed above that temperature effects could have been partially responsible for this phenomenon. However, since such a decline was also observed at constant temperatures during grow-out experiments in the Arabian Sea, it is worth analysis in this context. The observed simple saturation patterns for other autotrophs can be attributed to the establishment of a balance between a predator and a prey: At high TChl *a* the predator's carrying capacity is set by prey biomass which no longer increases as TChl *a* increases. However, the cell size of *Prochlorococcus* is similar to the size of marine heterotrophic bacteria and it is likely that

some herbivores that graze on *Prochlorococcus*, e.g., heterotrophic or mixotrophic flagellates or ciliates (Christaki et al. 1999; Guillou et al. 2001; Frias-Lopez et al. 2009), also graze on heterotrophic bacteria (fig. 8C). The biomass of bacteria is expected to increase as total autotroph biomass increases, since all autotrophs directly or indirectly produce dissolved organic carbon on which bacteria depend for growth (fig. 8D). Thus, the biomass of bacterial grazers is expected to increase with TChl *a* as well. Since it is likely that these also graze on *Prochlorococcus*, grazing pressure on *Prochlorococcus* is expected to increase with increasing autotroph biomass, even if *Prochlorococcus* biomass has leveled off. A consequence of the increasing grazing pressure and constant division rates will be a decline of the biomass of *Prochlorococcus* at high TChl *a*, as observed in the field data (fig. 5). Thus, the decline in the abundance of *Prochlorococcus* with larger values of TChl *a* is likely due to a decoupling of predator-prey dynamics between *Prochlorococcus* and its grazers due to the availability of other prey for these.

To conclude, this study has both important practical and theoretical implications. The observed patterns allow us to predict the response of phytoplankton communities to changes in ocean climate, for example those associated with global climate change. Those predictions are more akin to predictions of ecological climate rather than forecasts of ecological dynamics. An important theoretical implication is the empirical confirmation of Thingstad's (1998) model at the level of taxonomic groups. These results suggest that forcing of phytoplankton community structure by either bottom-up or top-down forces does not occur. Phytoplankton community structure is controlled by a balance between those, and likely other, forces. The results also imply that the microbial loop in places covered by this study is mostly at a steady state that varies in a predictable manner with rates of nutrient input to the system. Data based on rate measurements, not only standing stocks of biomass, that support these arguments were also presented by Goericke & Welschmeyer (1998) and Goericke (2002). These conclusions support the arguments of Banse (1992; 1995) and Verity and Smetacek (1996), who have argued that predation is a powerful, and often neglected, force in the marine environment.

## ACKNOWLEDGMENTS

I am grateful to the crews of the R/V *Revelle* and *New Horizon* for support at sea, Amy Shankle, Maria Mendez and Connie Fey for pier sampling, and to Jason Pearl for help in the lab. K. Banse, M. Roadman, B. Palenik, E. Venrick and three anonymous reviewers are thanked for their critical and helpful comments on the manuscript. The research was supported by a grant from ONR (N00014-98-1-005) and NSF (OCE-01018038).

## LITERATURE CITED

Anderies, J. M., and B. E. Beisner. 2000. Fluctuating environments and phytoplankton community structure: A stochastic model. Am. Nat. 155:556–569.

Anderson, C. R., D. A. Siegel, M. A. Brzezinski, and N. Guillocheau. 2008. Controls on temporal patterns in phytoplankton community structure in the Santa Barbara Channel, California. J. Geophys. Res.-Oceans 113:16.

Banse, K. 1982. Mass-scaled rates of respiration and intrinsic growth in very small invertebrates. Mar. Ecol. Prog. Ser. 9:281–297.

Banse, K. 1992. Grazing, temporal changes in phytoplankton concentrations, and the microbial loop in the open sea, p. 409–440. *In* P. G. Falkowski and A.D. Woodhead [eds.], Primary productivity in the sea. Plenum.

Banse, K. 1995. Zooplankton: Pivotal role in the control of ocean production. ICES J. mar. Sci. 52:265–277.

Bissett, W. P., J. J. Walsh, D. A. Dieterle, and K. L. Carder. 1999. Carbon cycling in the upper waters of the Sargasso Sea: I. Numerical simulation of differential carbon and nitrogen fluxes. Deep-Sea Res. I 46:205–269.

Brown, S. L. and others 2002. Microbial community dynamics and taxon-specific phytoplankton production in the Arabian Sea during the 1995 monsoon seasons. Deep-Sea Res. II 49:2345–2376.

Campbell, L., H. A. Nolla, and D. Vaulot. 1994. The importance of *Prochlorococcus* to community structure in the central North Pacific Ocean. Limnol. Oceanogr. 39:954–961.

Chisholm, S. W. 1992. Phytoplankton size, p. 213–237. *In* P. G. Falkowski and A. D. Woodhead [eds.], Primary productivity and biogeochemical cycles in the sea. Plenum.

Chisholm, S. W. and others. 1992. *Prochlorococcus marinus* nov. gen. nov. sp.: an oxyphototrophic marine prokaryote containing divinyl chlorophyll *a* and *b*. Arch. Microbiol. 157:297–300.

Christaki, U. and others. 1999. Growth and grazing on *Prochlorococcus* and *Synechococcus Limnol Oceanogr* 44:52–61.

Claustre, H. 1994. The trophic status of various oceanic provinces as revealed by phytoplankton pigment signatures. Limnol. Oceanogr. 39:1206–1210.

Denman, K. L. 2003. Modelling planktonic ecosystems: parameterizing complexity. Prog. Oceanogr. 57:429–452.

Ewart, C. S. and others. 2008. Microbial dynamics in cyclonic and anticyclonic mode-water eddies in the northwestern Sargasso Sea. Deep-Sea Research Part Ii-Topical Studies in Oceanography 55:1334–1347.

Fenchel, T., and B. J. Finlay. 1983. Respiration rates in heterotrophic, free-living protozoa. Microb. Ecology 9:99–122.

Francois, R. and others. 1993. Changes in the $\delta^{13}C$ of surface water particulate organic matter across the subtropical convergence in the S. W. Indian Ocean. Global Biogeochem. Cycles 7:627–644.

Franks, P. J. S. 2001. Phytoplankton booms in a fluctuating environment: the roles of plankton response time scales and grazing. J. Plank. Res. 23:1433–1441.

Frias-Lopez, J., A. Thompson, J. Waldbauer, and S. W. Chisholm. 2009. Use of stable isotope-labelled cells to identify active grazers of picocyanobacteria in ocean surface waters. Environ. Microbiol. 11:512–525.

Friedrichs, M. A. M. and others. 2007. Assessment of skill and portability in regional marine biogeochemical models: Role of multiple planktonic groups. J. Geophys. Res.-Oceans 112:22.

Geider, R. J., H. L. Mcintyre, and T. M. Kana. 1996. Dynamic model of phytoplankton growth and acclimation: Responses of the balanced growth rate and the chlorophyll *a* : carbon ratio to light, nutrient-limitation and temperature. Mar. Ecol. Prog. Ser. 148:187–200.

Goericke, R. 1998. Response of phytoplankton community structure and taxon-specific growth rates to seasonally varying physical forcing at a station in the Sargasso Sea off Bermuda. Limnol. Oceanogr. 43:921–935.

Goericke, R. 2002. Top-down control of phytoplankton biomass and community structure in the monsoonal Arabian Sea. Limnol. Oceanogr. 47:1307–1323.

Goericke, R. 2011. The size structure of marine phytoplankton communities—What are the rules? CalCOFI Reports in press.

Goericke, R., and J. Montoya. 1998. Estimating the contribution of microalgal taxa to chlorophyll *a* in the field–variations of pigment ratios under nutrient- and light-limited growth. Mar. Ecol. Prog. Ser. 169:97–112.

Goericke, R., R. J. Olson, and A. Shalapyouok. 2000. A novel niche for *Prochlorococcus* sp. in low-light suboxic environments in the Arabian Sea and the Eastern Tropical North Pacific. Deep-Sea Res. I 47:1183–1205.

Goericke, R., and N. A. Welschmeyer. 1998. Response of Sargasso Sea phytoplankton biomass, growth rates, and primary production to seasonally varying physical forcing. J. Plankton Res. 20:2223–2249.

Guillou, L., S. Jacquet, M. J. Chretiennot-Dinet, and D. Vaulot. 2001. Grazing impact of two small heterotrophic flagellates on *Prochlorococcus* and *Synechococcus*. Aquat. Microb. Ecol. 26:201–207.

Hulburt, E. M., J. M. Ryther, and R. R. L. Guillard. 1960. The phytoplankton of the Sargasso Sea off Bermuda. J. Con. Int. Explor. Mer. 25:115–128.

Jeffrey, S. W., R. F. C. Mantoura, and S. W. Wright. 1997. Phytoplankton pigments in oceanography. UNESCO Publishing.

Latasa, M., M. R. Landry, L. Schlüter, and R. R. Bidigare. 1997. Pigment-specific growth and grazing rates of phytoplankton in the equatorial Pacific. Limnol. Oceanogr. 42:289–298.

Letelier, R. M. and others. 1993. Temporal variability of phytoplankton community structure based on pigment analysis. Limnol. Oceanogr. 38:1420–1437.

Li, W. K. W. 2002. Macroecological patterns of phytoplankton in the northwestern North Atlantic Ocean. Nature 419:154–157.

Litchman, E. and others. 2006. Multi-nutrient, multi-group model of present and future oceanic phytoplankton communities. Biogeosciences 3:585–606.

Macintyre, J. G., J. J. Cullen, and A. D. Cembella. 1997. Vertical migration, nutrition and toxicity in the dinoflagellate *Alexandrium tamarense*. Mar. Ecol. Prog. Ser. 148:201–216.

Mackey, M. D., D. J. Mackey, H. W. Higgins, and S. W. Wright. 1996. CHEMTAX—a program for estimating class abundances from chemical markers: application to HPLC measurements of phytoplankton. Mar. Ecol. Prog. Ser. 144:265–283.

Malone, T. C. 1971. The relative importance of nanoplankton and netplankton as primary producers in tropical oceanic and neritic phytoplankton communities. Limnol. Oceanogr. 16:633–639.

Margalef, R. 1978. Life-forms of phytoplankton as survival alternatives in an unstable environment. Oceanol. Acta 1:493–509.

May, R. M. 1981. Models for two interacting populations, p. 78–104. *In* R. M. May [ed.], Theoretical Ecology. Sinauer Assoc.

Menzel, D. W., and J. H. Ryther. 1960. The annual cycle of primary production in the Sargasso Sea off Bermuda. Deep-Sea Res. 6:351–367.

Michaels, A. F., and M. W. Silver. 1988. Primary production, sinking fluxes and the microbial food web. Deep-Sea Res. 35:473–490.

Moore, J. K. and others. 2002. An intermediate complexity marine ecosystem model for the global domain. Deep Sea Research II 403–462.

Mullin, M. M. 1998. Biomasses of large-celled phytoplankton and their relation to the nitricline and grazing in the California Current system off Southern California, 1994–1996. CalCOFI Reports 39:117–123.

Mullin, M. M. 2000. Large-celled phytoplankton, the nitricline, and grazing during the California 1997–98 El Niño. CalCOFI Reports 41:161–166.

O'neill, R. V., D. L. Deangelis, J. B. Waide, and T. F. H. Allen. 1986. A hierarchical concept of ecosystems. Princeton Univ. Press.

Raimbault, P., M. Rodier, and I. Taupier-Letage. 1988. Size fraction of phytoplankton in the Ligurian Sea and the Algerian Basin (Mediterranean Sea): Size distribution versus total concentration. Mar. Microb. Food Webs 3:1–7.

Scripps Institution of Oceanography. 1997. Physical, Chemical and Biological Data, CalCOFI cruises 9607 and 9610.

Sheldon, R. W., W. H. Sutcliffe, Jr., and M. A. Paranjape. 1977. Structure of pelagic food chain and relationship between plankton and fish production. J. Fish. Res. Board Can. 34:2344–2353.

Smayda, T. J. 1980. Phytoplankton species succession, p. 493–570. *In* I. Morris [ed.], The physiological ecology of phytoplankton. Blackwell.

Smetacek, V. 1999. Diatoms and the ocean carbon cycle. Protist 150:25–32.

Sprules, W. G., and M. Munawar. 1986. Plankton size spectra in relation to ecosystem productivity, size, and perturbation. Can. J. Fish. Aquat. Sci. 43:1789–1794.

Steinberg, D. K. and others. 2001. Overview of the US JFOFS Bermuda Atlantic Time-series Study (BATS): a decade-scale look at ocean biology and biogeochemistry. Deep-Sea Res. II 48:1405–1447.

Thingstad, T. F. 1998. A theoretical approach to structuring mechanisms in the pelagic food web. Hydrobiologia 363:59–72.

Tyrrell, T., P. Holligan, and C. Mobley. 1999. Optical impacts of oceanic coccolithophore blooms. J. Geophys. Res. 104:3223–3242.

Venrick, E. L. 1982. Phytoplankton in an oligotrophic ocean: observations and questions. Ecol. Monogr. 52:129–154.

Venrick, E. L. 2002. Floral patterns in the California Current System off southern California: 1990–1996. J. Mar. Research 60:171–189.

Verity, P. G., and V. Smetacek. 1996. Organism life cycles, predation, and the structure of marine pelagic ecosystems. Mar. Ecol. Prog. Ser. 130:277–293.